Evaluation of Mechanical and Thermal Properties of Alkali-Treated Sisal, Bamboo, and Hybrid Fiber-reinforced Polymer Composites

Mihiretu Gezahagn Ganta
Department of Mechanical Engineering, Wolaita Sodo University

Patel, Mahaboob
Department of Mechanical Engineering, Wolaita Sodo University

https://doi.org/10.5109/7236831

出版情報：Evergreen. 11 (3), pp.1784-1797, 2024-09. Interdisciplinary Graduate School of Engineering Sciences, Kyushu University, Japan
バージョン：

Evaluation of Mechanical and Thermal Properties of Alkali-Treated Sisal, Bamboo, and Hybrid Fiber-reinforced Polymer Composites

Mihiretu Gezahagn Ganta[1,2,*], Mahaboob Patel[1]
[1]Department of Mechanical Engineering, Wolaita Sodo University, Wolaita Sodo, Ethiopia
[2]Faculty of Mechanical Engineering, Opole University of Technology, Opole, Poland

*Author to whom correspondence should be addressed:
E-mail: mihiretu.gezahagn@wsu.edu.et

(Received November 10, 2023: Revised May 31, 2024: Accepted June 21, 2024).

Abstract: Composites have limitless engineering applications where strength-to-weight ratio, low cost, and ease of manufacture are needed. This study presents to synthesize and evaluate the mechanical and thermal properties of sisal, bamboo, and hybrid fiber-reinforced composites. Combined chemical and enzyme-assisted extraction methods were employed to extract bamboo fibers, while sisal fibers were extracted using a fiber-extracting machine. Due to the variations in lignin, hemicelluloses, pectin, and wax content and strength among natural fibers, both fibers were subjected to different concentrations of treatments over varying periods. Composites were fabricated using the hand lay-up method considering 0, 45, and 90-degree fiber ply orientation angles. Unsaturated polyester mixed with Methyl ethyl ketone peroxide is used as a matrix. From the experimental analysis, it has been identified that bamboo fiber-reinforced composites exhibited 140.17 MPa tensile strength with a maximum tensile modulus of 2,595.74 Pa. The variation in tensile strength was significantly affected by the fiber orientation, whereas the compressive strength was influenced by both the fiber type and orientation. As a sample is continually weighted while heating, the bamboo fiber-reinforced composites had a lower mass change and thus, are thermally stable compared to sisal and hybrid composites. ANOVA results for tensile and compressive strength showed that fiber orientation contributed 83.79% for tensile strength and 47.38 % for compressive strength, whereas fiber type contribution was 5.23% and 46.97 %, respectively. Intending to utilize natural fiber-reinforced composites in applications requiring both structural and thermal stability, the study contributes to the advancement of environmentally friendly materials for the applications prioritizing environmental sustainability and technological innovation.

Keywords: Bamboo fiber; Hybrid fiber; Mechanical property; Sisal fiber; Thermal property

1. Introduction

Metals, alloys, and ceramics are unable to attain the ideal amalgamation of equipment properties required by modern technology; notably in transportation, aeronautics, submarine, and energy applications[1,2]. Manufacturers and scientists are under increased pressure to investigate new, viable, and eco-friendly materials to replace the existing synthetic and glass-based composite materials and to bring down credence on petroleum-based products[3,4]. Composite materials enable us to acquire the desired characteristics by strategically combining two or more materials. Natural fibers such as banana, coir, sisal, and bamboo fibers have been used to make composites for retail goods, low-cost bodies, and other civil structures[5,6]. In another way, industrial waste materials have been utilized as reinforcing agents due to their ability to easily integrate with thermoplastic or thermoset matrices, enhancing composite materials' thermal, mechanical, and tribological properties[7]. Blast Furnace Slag, Red Mud, Fly Ash, waste Glass, and Linz Donawitz Slag are widely used industrial wastes[7-10]. The inclusion of these waste materials resulted in improved properties of surface roughness, hardness, stiffness, flexural strength, and modulus[7,8]. The variability and unpredictability of waste composition significantly affect the consistency of material property and performance[9], posing challenges in medical applications and extreme environments. Natural fiber-reinforced composites (NFRCs) address this issue and are effectively employed in the medical and aerospace industries[2]. They are widely chosen due to their benefits of being lightweight, low cost, having good specific properties, and being eco-friendly and biodegradable[11]. They possess high specific strength, non-abrasive properties, acoustic insulating characteristics, and high resistance to corrosion[12]. However, these NFRCs have compatibility issues due to the hydrophilic nature of fibers and the hydrophobic properties of the matrices. Consequently, it is necessary to use coupling agents to ameliorate the adhesion between the matrix and reinforcement[13]. Natural fibers (NFs) are categorized as animal and plant fibers corresponding to their genesis. Jute, coir, sisal, pineapple, bamboo, and ramie fibers fall under the category of plant fibers[14]. Sisal fiber (SF) is a strong, stiff fiber that can grow in dry and sweltering conditions, often unsuitable for other plants[15]. The performance of natural composite material is improved by chemically treating the fibers to enhance the adhesion between the fiber and matrix. Strong bonding and superior mechanical properties were obtained with chemically treated sisal fiber-reinforced composites compared to the untreated ones[16-19]. Bamboo fibers (BFs) extracted from bamboo plants have excellent characteristics and have been used in a wide variety of applications; their rapid growth, environmental benefits, and excellent mechanical properties have drawn significant research interest[20,21]. The characteristics of NFRC were thoroughly assessed by Lokesh *et al.*[22]. Hand lay-up and compression manufacturing methods were used to fabricate the composites with treated and untreated bamboo fibers. The fiber content and fiber length effect on mechanical properties were studied and the optimum properties were found with treated fibers at 30wt% of fiber content[22]. The mechanical properties of sisal fiber reinforced composite have been studied by Betelie *et al.*[23]; the fibers were soaked in NaOH solution for 3 hours and washed with distilled water to clean the traces of NaOH. The result revealed that the maximum tensile and flexural strengths were found at 30wt% of fiber to matrix ratio. Ragunath *et al.*[24] studied the mechanical properties of hybrid fiber-reinforced composites using sisal and glass fibers. According to their findings, sisal fiber had the most profound impact on tensile and impact strength properties; this has been also confirmed by ANOVA with a <0.05 significance level. Based on regression analysis, Wang *et al.*[25] investigated the thermal and mechanical properties of bamboo fiber-reinforced composite. Casts were made using compression molding and needle-punching processes. Their findings demonstrated the potential of regression analysis to create a causal connection between the employed parameters and anticipated outcomes. Both the transverse and longitudinal breaking strengths of the composite decreased with increased wt% of BFs[25]. As diverse characteristic fibers were utilized while fabricating composites, it is necessary to distinguish likenesses and contrasts of composites based on their mechanical and thermal properties. The current research work uses a machine-assisted extraction method to obtain sisal fibers and combined chemical and enzyme-assisted extraction methods to extract bamboo fibers. The focus of this research is on the experimental characterization of the mechanical and thermal properties of sisal, bamboo, and hybrid fiber-reinforced composite materials, which contributes significantly to understanding the mechanical properties, thermal stability, and energy absorption potential of composite materials. Consequently, it holds immense importance for promoting sustainability and enhancing the performance of natural composite materials.

2. Materials and Methods

2.1 Materials

Unsaturated polyester resin (UPR) was supplied with a cobalt naphthenate accelerator from World Glass Fiber PLC, Ethiopia. An organic methyl ethyl ketone peroxide (MEKP) catalyst was used as a curing agent. The matrix was selected due to its advantages of low cost, resistance to chemicals and weathering, and low shrinkage during the curing process[26-28]. Sisal and bamboo fibers are chosen owing to their numerous advantages over other natural fibers[29]. An adequate quantity of three-year-old "Agave sisalana" and three-and-a-half-year-old "Oxytenantheria abyssinica" species of sisal and bamboo plants were collected from the Wolaita and Gedeo zones, Ethiopia, respectively. The chemical composition, physical and mechanical properties of both sisal and bamboo fibers are presented in Table 1. A highly caustic inorganic sodium hydroxide (NaOH) compound in the form of flakes was used for cleaning and bleaching the surface of plant fibers. A special gleam paste honey wax mold release was used as a releasing agent. A mild steel mold with base and lid parts was manufactured with an internal dimension of 350 mm x 3500 mm. This particular dimension is chosen to eliminate the possible dimensional instability of the mold during the loading and curing process. A thin plastic sheet and a self-made wood roller were used to facilitate the easy removal of composite casts and the proper spreading of the matrices.

Table 1. Properties of sisal and bamboo fibers[30,31]

Properties		SF	BF
Physical and Mechanical	Density (g/cm^3)	1.33-1.5	0.6-1.1
	E (GPa)	9.0-38.0	11-32
	TS (MPa)	400-700	140-800
	εB (%)	2.0–2.50	4.65
Chemical composition	Lignin (%)	9.90	21-31
	Hemicelluloses (%)	12.0	30.0
	Cellulose (%)	65.0	26-43
	Wax (%)	2.0	-
	Moisture content (%)	8.90	8.80

Note: εB, E, and TS represent elongation at break, Young's modulus, and tensile strength respectively.

2.2. Methods

2.2.1. Fiber extraction

Owing to difficulties related to bamboo fiber extraction[32,33], in this study the BFs were drawn out from the pseudo-stem of bamboo plant with the combined chemical and enzymatic extraction process. The procedure followed begins with cutting and dissecting bamboo internodes as shown in Fig. 1('a'1 and 'a'2). The solution of 20 mg/ml pectase, 15 mg/ml hemicellulose, and 20 mg/ml lignoenzyme enzymes were prepared; and the dissected bamboo fibers were submerged in this mixture and kept for 2 days at room temperature as shown in Fig. 1('a'3 and 'a'4). The rotted bamboo strips were removed from the enzyme mixture and soaked in 6% mass over a volume of NaOH for 48 hours to influence hemicellulosic and lining parts, Fig. 1('a'5). The soaked strips are removed from the NaOH solution and washed slightly with distilled water, Fig. 1('a'6). Finally, the fibers were cleaned with a 0.2N sodium solution and dried for 4 days at room temperature as shown in Fig. 1('a'7 and 'a'8). During the sisal fiber extraction process, after cutting and removing thorns from the base and tip of the leaf, the fibers were extracted with the help of the sisal fiber extraction machine, Fig. 1 ('b'1); and the decorticated fibers were cleaned with distilled water as shown in Fig. 1 ('b'2). As the amount of moisture content influences the fiber quality, the extracted and cleaned fibers were dried at room temperature for 3 days as shown in Fig. 1 ('b'3).

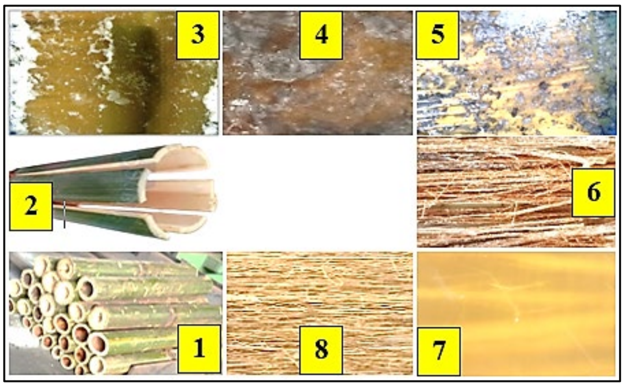

'a'

'b'

Fig. 1: Fiber extraction process; 'a' BFs and 'b' SFs

2.2.2. Alkaline treatment

Alkali treatment (AT) is the most preferred treatment for natural fibers, which significantly improves the interfacial adhesion between fiber and matrix[34]. Owing to different concentrations of lignin, hemicelluloses, pectin, and wax content and strength between sisal and natural fibers, both fibers were subjected to different concentrations of treatments over varying periods. In this study, as shown in Fig. 2, BFs were soaked in 6% mass over a volume of NaOH for 8 hours. This method was repeated with 5%, 4%, and 3% mass over a volume of NaOH for 3, 2, and 1 hours, respectively under 75 °C. Finally, the fibers were washed with 0.2N sodium solution and dried outdoors for 4 days. Moreover, a 6% and 2.5% NaOH solution was used to treat sisal fibers. As shown in Fig. 3, the fibers were soaked for about 4 and 2 hours at 82 °C respectively. To get rid of the excess NaOH adhering, the fibers were rinsed with adequate water. Lastly, the fibers were dried outdoors for three days. As presented in Fig. 2'c' and 'd', it is apparent that as the treatment progresses, the intensity of waxes and lignin decreases; towards the end, the color of the removed liquids took on a slight turquoise color. However, excessive treatment could potentially weaken the strength of fibers. On the other hand, as demonstrated in Fig. 3, treating SFs followed by cleaning at each step with a water enhanced the effectiveness of subsequent treatments.

Fig. 2: Alkali treatment of BF: a) NaOH flakes, b) measuring of BF, c) and d) removed impurities after AT

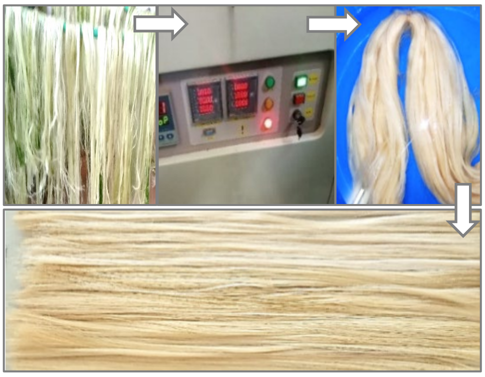

Fig. 3: Alkali treatment of sisal fibers

2.2.3. Weight and volume fraction

The fiber volume fraction (Vf_{fiber}) and weight fraction (Wf_{fiber}) are important mathematical elements in composite engineering. They represent the percentage of fiber volume and mass in the entire volume (Vc) or mass (Mc) of composites. The densities of the reinforcement materials used are 1.3 g/cm^3 and 1.50 g/cm^3 for bamboo and sisal fibers, respectively; and the matrix densities are 1.22 g/cm^3 and 1.17 g/cm^3 for polyester and MEKP, respectively. The matrix reaction starts with the addition of 5% MEKP. While computing the volume/mass fraction, the density of the catalyst was neglected. Furthermore, the density of the composite panel is computed by performing the ratio of mass to volume. The hybrid fiber was made with 50% sisal and 50% bamboo fibers. Mono and hybrid fiber-reinforced composites are fabricated with a 30 wt% of fiber-to-matrix ratio. The corresponding volume and weight fractions are presented in Table 2.

2.2.4. Taguchi design of experiment (Taguchi DOE)

Taguchi DOE is designed to provide an independent evaluation of factors through a small number of trials to achieve the best response. It is used to reduce the variation in outputs caused by uncontrollable factors and to identify the optimal factor settings that will result in robust and reliable performance. For this research work, two factors and three levels are considered with the L9 orthogonal array (OA), as shown in Table 3. The selection of fiber orientation as a factor is crucial due to its significant impact on the load-bearing capacity, anisotropy, and overall behavior of the composite material. The current research work with this valuable information can be utilized to effectively guide the manufacturing process and design of composite structures, enabling them to meet specific requirements and achieve the desired performance characteristics.

Table 2. Volume and mass fraction of sisal, bamboo, and hybrid fiber-reinforced composites (HFRC)

Fibers	Vc (cm^3)	Density (ρc) of composite (g/cm^3)	Mc (g)	Fiber mass (g)	Wf_{fiber}	Fiber volume (cm^3)	Vf_{fiber}
BFs	821.4	1.1813	970.31	291.09	0.299	264.62	0.322
SFs	821.4	1.2923	1061.49	318.44	0.299	212.29	0.258
HFs	821.4	1.2429	1020.91	306.27	0.299	235.59	0.286

Table 3. 'a' coding matrix, 'b' design matrix and composite designations

'a'

Runs	Factors A	Factors B
1	1	1
2	1	2
3	1	3
4	2	1
5	2	2
6	2	3
7	3	1
8	3	2
9	3	3

'b'

Runs	Factors: Fibers	Factors: Orientation	Composite designation
1	SF	0-degree	SFRC0
2	SF	45-degree	SFRC45
3	SF	90-degree	SFRC90
4	BF	0-degree	BFRC0
5	BF	45-degree	BFRC45
6	BF	90-degree	BFRC90
7	HF	0-degree	HFRC0
8	HF	45-degree	HFRC45
9	HF	90-degree	HFRC90

2.3. Composite fabrication

UPR and MEKP catalyst were mixed at a 20:1 weight ratio at room temperature for 2 minutes. The composite fabrication steps as shown in Fig. 4 includes preparing the matrix reaction, followed by placing a thin plastic sheet on the mild steel mold. Next, honey wax mold release was applied on a plastic sheet, which is placed on the face of

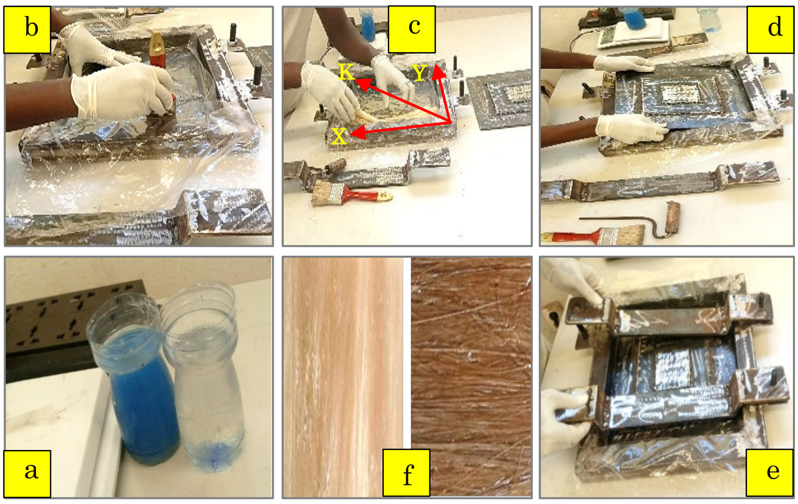

Fig. 4: Steps involved in composite fabrication: a) matrix before measuring, b) Applying honey wax, c) laying pre-impregnated fibers, d) placing top sheet and cover, e) fixing of cover before load f) cured composites.

both base and lid parts of the mold. Laying down pre-impregnated fibers with a mixed matrix was the middle stage, which was followed by fixing the fixtures on all sides with 166.77 N-applied dead weight (i.e. loading a 17 kg dead weight on the lid plate). When producing a composite with fibers oriented at 45 degrees, instead of putting the fibers at 45-degree angle in the mold, the mold itself was tilted to 45-degree angle, allowing the fibers to be placed as they would be for 0 and 90-degree orientations by considering 'K' as a reference axis as shown in Fig. 4c. To eliminate the possible orientation error, the mold was manufactured with a 90-degree angle in all corners, and the protractor was used to tilt the mold into a 45-degree angle. As illustrated in Fig. 4c, the composite manufacturing procedures with 90 and 0-degree fiber alignment began in the X and Y directions, respectively. This assures that all fibers stick to the angle defined by the end of the mold.

2.4. Sample preparation

Following the fabrication of nine composite casts with a 6 mm thickness, the specimens were prepared for each mechanical and thermal analysis following ASTM D3039 standards for tensile and ASTM D3410 for compressive strength tests. Given that the dimensions of the samples and the occurrence of cracks and necks during sample preparation can significantly influence the mechanical properties of composites, the shaping of samples was done using a WEN 3922 scroll saw machine. The thermal analysis of the composite materials was conducted using a DTG-60H detector under a nitrogen atmosphere with a flow rate of 50 ml/min. A superfine coarse-grain pulverizer stainless screw was used to manually prepare the samples for thermal analysis. To maintain consistency, a constant sample weight of 10.129 mg and a molecular weight of 0.00 gram/mol were employed for all samples.

3. Result and Discussion

The force required to break a polymer composite specimen and the amount to which the specimen extends to that breaking point was measured using the ASTM D3039 tensile test. Specimens are held in a grasp of Universal Testing Machine (UTM) and pulled until the material breaks as shown in Fig. 5 'a'. The ASTM D3410 compression test method was used to determine the compressive strength of fiber-reinforced composites. Opposing forces are applied to the specimen to squash or flatten it as presented in Fig. 5 'b'. The test speed was taken as 0.5 mm/min for both tests.

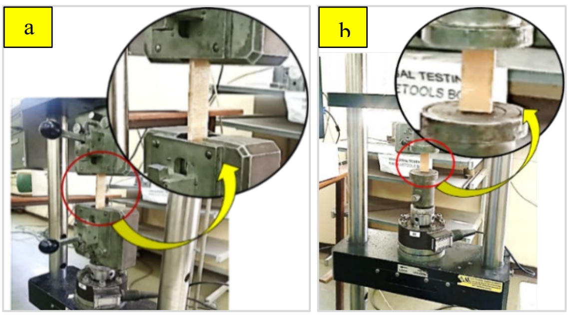

Fig. 5: Specimen under a) tensile test and b) compressive test

3.1. Tensile test

The tensile test result indicates that the employed factors and their levels exhibited a significant impact on the mechanical properties of composites, particularly on tensile strength and modulus. When comparing different fiber types (SFs, BFs, and HFs), it is observed that bamboo fiber-reinforced composites exhibited the highest tensile strength with a maximum value of 62.92 MPa as shown in Table 4. This result demonstrates that the fiber types employed for the production of fiber-reinforced composites influenced their overall tensile strength; however, the variation in tensile strength in 0 and 45 degrees of fiber orientation was not statistically significant. Furthermore, the study reveals interesting trends in the relationship between fiber orientation and tensile strength. The tensile strength of sisal fiber reinforced composite (SFRC) increased by 80.68% when the fiber orientation changed from 0 to 45 degrees, and an even more impressive improvement (i.e. 809.25%) was exhibited when the orientation changed from 45 to 90 degrees. This emphasizes the importance of considering the optimal fiber orientation to achieve the desired strength level.

Table 4. Maximum tensile strength and Modulus

Specimens	Maximum tensile strength (MPa)	Maximum output force (kN)	Maximum tensile modulus (Pa)
SFRC0	3.83	0.46	335.821
SFRC45	6.92	0.83	263.087
SFRC90	62.92	7.55	890.323
BFRC0	4.08	0.49	242.857
BFRC45	6.00	0.72	276.238
BFRC90	140.17	16.82	2595.74
HFRC0	3.99	0.48	1333.33
HFRC45	8.75	1.05	595.238
HFRC90	85.08	10.21	1688.10

As presented in Fig. 6, all composites fabricated with 0-degree orientation demonstrated lower tensile strength. This is due to the fact that in fiber-reinforced composites, the fibers are the primary load-bearing components due to their high tensile strength and stiffness. Aligning the fibers to the applied load direction enables the fibers to efficiently carry the applied load. Contrarily, in the case of 0-degree orientation, when fibers are aligned perpendicularly to the load direction, the matrix material bears most of the load. The tensile strength of composites in this group is found to be smaller because the matrix often exhibits considerably less stiffness and tensile strength compared to the fibers. In the composite with perpendicular fiber arrangement to the applied load, shear stresses occur at the matrix-fiber interface. In contrast to 0-degree and 90-degree orientations, the tensile strength of fiber-reinforced polymer composites varies when the fibers are orientated at a 45-degree angle to the normal direction of load. Samples from this group resulted in shear failure modes because the transferred load into the composite decomposed into axial and shear components. The parallel force component causes axial stress in fibers while the perpendicular one induces shear stress within the matrix and fiber interface. The induced considerable shear stress at the interface resulted in interfacial debonding or slipping even with lower loads.

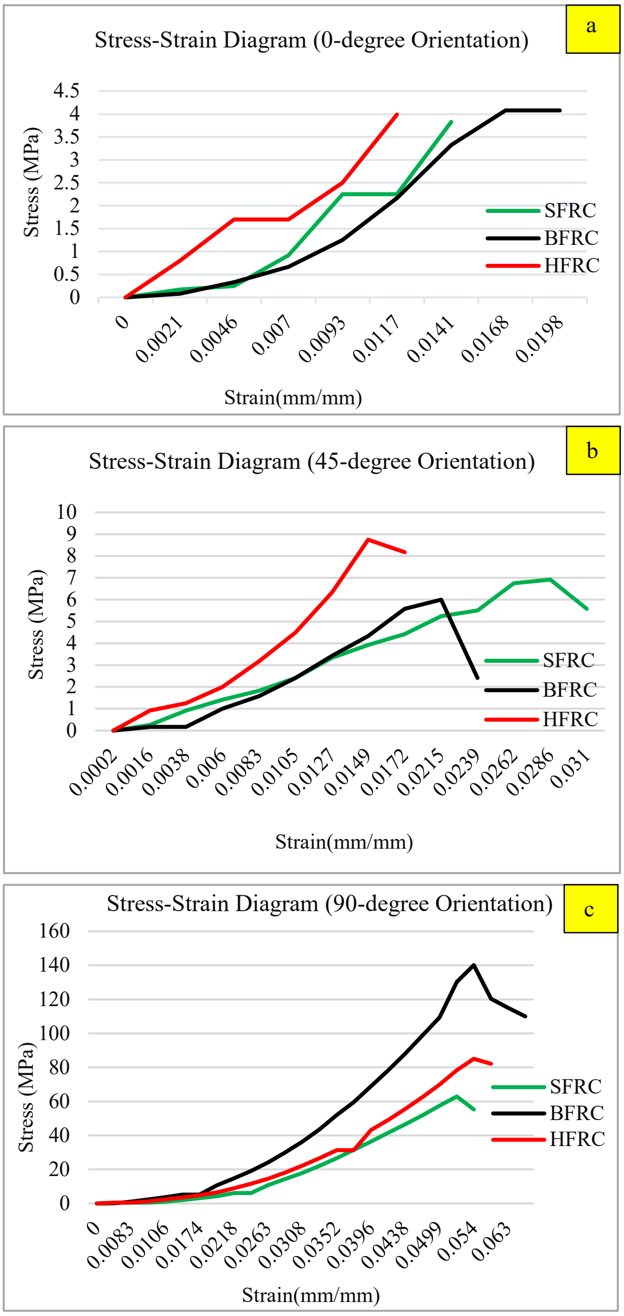

Fig. 6: Tensile test engineering stress-strain diagram of SFRC, BFRC, and HFRC for (a) 0-degree (b) 45-degree and (c) 90-degree orientation

The observed failure mechanism in this group includes fiber buckling/kinking, interfacial debonding, and matrix cracking which will be discussed in section 3.7. The stress distribution in this group of composite is anisotropic with both shear and normal stresses. As a result, the tensile strength of composites with 45-degree orientation is higher than 0-degree oriented ones but exhibited lower value compared to 90-degree fiber orientation. In the case where fibers in a composite are aligned parallel to the direction of applied load (i.e. 90-degree orientation), the applied load is profoundly transferred to the primary load-bearing part (fibers). In this group, the high tensile properties of fiber and its stiffness are fully utilized. This resulted in efficient load-carrying capacity and enabled the composite specimens to exhibit the maximum tensile strength. This group of composite had a lower shear stress at the fiber-matrix interface as the applied load is primarily axial. This reduces the possible sliding and interfacial debonding failures, which are common failure mechanisms in 0 and 45-degree orientations. The observed failure mechanism in the composites with 90-degree fiber orientation was the fiber fracture. This mode of failure requires significantly higher stress compared to matrix cracking or interfacial debonding. This orientation allows the composite to achieve its highest possible tensile strength. The findings emphasize the importance of considering fiber orientation during designing and producing composite materials. The results provide valuable insights that can be used to optimize the fabrication process and achieve the desired performance characteristics.

3.2. Compression test

The compressive strength test results are compared in Table 5. The experimental result shows that the fiber type has a trivial effect on the variation of compressive strength compared to fiber orientations. This is demonstrated by BFRC0 and HFRC0, which have almost the same compressive strengths of 120.92 MPa and 120.08 MPa, respectively.

Table 5. Compressive strength and output force

Specimens	Compressive strength (MPa)	Output force (kN)
SFRC0	102.75	12.33
SFRC45	53.17	6.38
SFRC90	49.08	5.89
BFRC0	120.92	14.51
BFRC45	94.50	11.34
BFRC90	92.50	11.10
HFRC0	120.08	14.41
HFRC45	97.08	11.65
HFRC90	92.95	9.295

The increasing compressive strength is found with a decreasing angle of orientation. The compressive strength of BFRC0 (120.92 MPa) reduced to 94.50 MPa and 92.50

MPa when the fiber orientation was increased to 45 and 90-degree orientation respectively. SFRC0 has a compressive strength of 17.68% and 16.86% lower than BFRC0 and HFRC0 respectively. In another orientation group, HFRC with 45-degree fiber plies orientation has a compressive strength of 82.58% and 2.73% greater when compared to SFRC45 and BFRC45 respectively. Consequently, HFRC has emerged as the superior in a group of composites with a 45-degree fiber orientation.

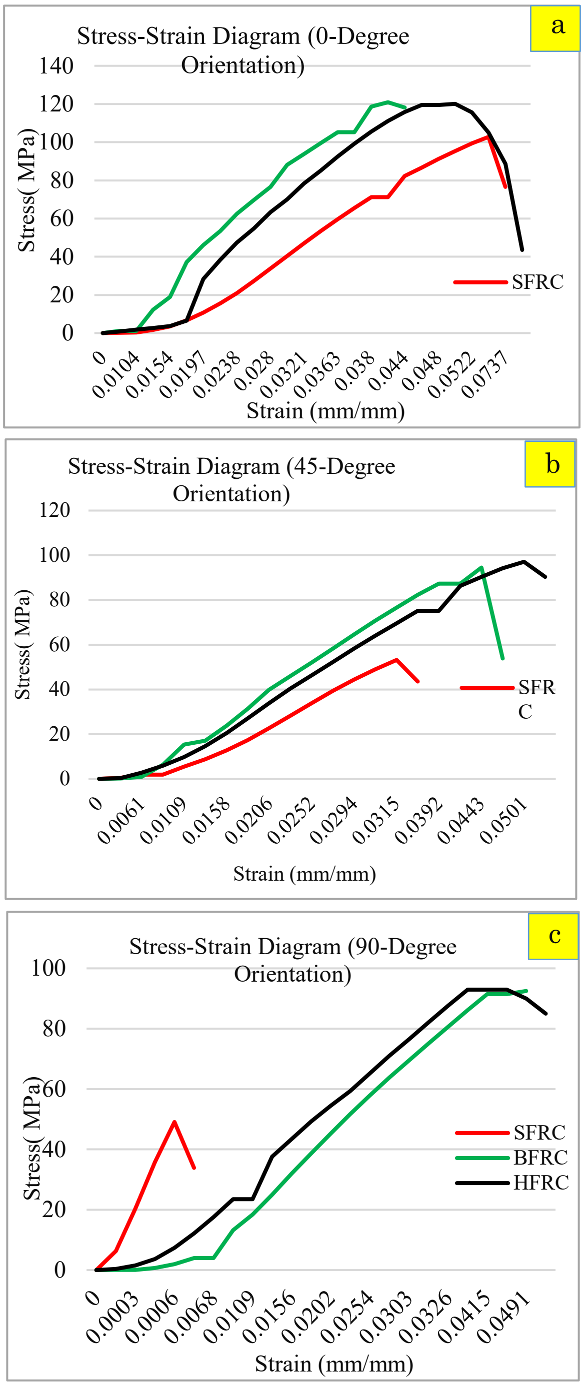

Fig. 7: Compression test engineering stress-strain diagram of SFRC, BFRC, and HFRC for (a) 0-degree (b) 45-degree and (c) 90-degree orientation

As shown in Fig. 7, BFRC0 attained a maximum compressive strength of 120.92 MPa with an applied load of 14.51 kN. Unlike tensile results, fiber orientation and fiber strengths are inversely proportional. For 90-degree orientation, where fibers are parallel to the compressive load direction, the compressive strength is generally lower. In this configuration, the matrix primarily bears the load as the fibers provide little resistance to compression. The matrix material, typically weaker and less stiff than the fibers, governs the compressive properties, leading to potential failure through matrix cracking or buckling under compressive stress. Additionally, the fibers experienced transverse compressive stresses, which resulted in micro-buckling and reduced the overall compressive strength. At 45-degree fiber orientation, the compressive strength of the composite is influenced by a combination of axial and shear stresses. The mixed stress state related with this particular fiber orientation contributed to various failure mechanisms, such as fiber kinking, matrix shearing, and interfacial debonding. As a result, the specimens in this group exhibited intermediate compressive strength compared to 0-degree and 90-degree orientations, benefiting from some fiber reinforcement but still limited by complex failure mechanisms. For a 0-degree orientation, where fibers are perpendicular to the compressive load direction, the composite exhibits the highest compressive strength. In this configuration, the collection of fibers directly resist the compressive load, leveraging their high strength. The matrix supports the fibers, preventing buckling and delamination, enhancing the overall stability of the composite under compression. This orientation effectively utilizes the compressive properties of both the fibers and the matrix, leading to higher compressive strength.

3.3. Analysis of variance (ANOVA)

ANOVA is a statistical technique for analyzing mean differences. It includes statistical models and the corresponding estimation methods (variation within and between groups). Table 6 shows that the fiber type used

Table 6. ANOVA for Tensile strength.

Source	DF	Adj SS	Adj MS	F	P	Ctr.(%)
Fibers	2	1022	510.9	0.95	0.459	5.23
Orientation	2	16383	8191.3	15.26	0.013	83.79
Error	4	2147	536.7			10.98
Total	8	19551				100.00

Note: Ctr. and DF represent the percentage of contribution and degree of freedom, respectively, which also applies to Table 7.

Table 7. ANOVA for Compressive strength.

Source	DF	Adj SS	Adj MS	F	P	Ctr.(%)
Fibers	2	2405.0	1202.52	16.61	0.012	46.97
Orientation	2	2426.1	1213.03	16.75	0.011	47.38
Error	4	289.7	72.42			5.66
Total	8	5120.8				100.00

for composite fabrication contributed 5.23% for tensile strength while the fiber orientation contribution was 83.79% with a 0.013 P-value, which is typically considered statistically significant. The finding suggests that the type of fiber used has a trivial effect on the variation of tensile strength compared to the fiber ply orientation. The error represents the differences or variations that cannot be explained by the factors or their levels being studied. Computing the interaction effect of fiber and orientation will minimize the percentage contribution of error. Considering compressive strengths' ANOVA, which is presented in Table 7, it was observed that, the orientation and fiber type contributed 47.38% and 46.97% respectively; this indicates that both the fiber type and orientation significantly affected corresponding compressive strength values. This is also confirmed by the corresponding P-value of 0.012 for fiber type and 0.011 for fiber orientation. Both values are >0.05, which indicates both factors significantly affected the compressive strength outcome.

3.4. Regression equation

The regression equation represents the relationship between the independent and dependent variables. It is typically written in the form;

$$Y = a + b1X1 + b2X2 + \ldots + bnXn$$

Where: 'Y' and $'a'$ represent the dependent variable and intercept respectively; and $X1, X2, \ldots, Xn$ represent the independent variables. The coefficients or slopes associated with each independent variable are represented by $b1, b2, \ldots, bn$. In this work, the specific values of the coefficients $(b1, b2, \ldots, bn)$ are obtained through the ANOVA analysis and indicate the strength and direction or sign of the relationship between each independent and dependent variable. The obtained regression equations for the tensile strength of each composite are obtained and presented in Table 8. The regression equation illustrates the fact that the orientation coefficient is positive to all regression equations of tensile test, which indicates that the tensile strength is directly proportional to the fiber ply orientations. The increase of fiber orientation angle from 0 to 90 degrees resulted in increased tensile strength. While the reverse trend is observed in compressive strength. As shown in Table 8, the independent variable coefficients are negative, proving that the compressive strength is inversely proportional to fiber ply orientation. This shows that increasing the fiber orientation resulted in decreasing the compressive strength.

Table 8. Regression equation

	Tensile	Compression
SFRC	-21.5 + 1.023 Orientation	86.54 - 0.405 Orientation
BFRC	4.0 + 1.023 Orientation	120.84 - 0.405 Orientation
HFRC	-13.4 + 1.023 Orientation	121.57 - 0.405 Orientation

3.5. Thermogravimetric analysis (TGA) and Differential thermal analysis (DTA)

TGA is a method of thermal analysis in which the mass of a sample is measured over time as the temperature changes[35]. In DTA, the material under study and an inert reference material are made to undergo identical thermal cycles while recording any temperature difference between the sample and reference[36]. The experimental results of TGA and DTA values at each peak and temperature level are presented in Table 9. Mono and hybrid composite samples were tested using DTG-60 instrument equipped with TA-60 thermal analysis workstation and FC-60A flow control unit. Pure nitrogen gas was used to clean the chamber to avoid oxidation and falsification of the results. SFRC, BFRC, and HFRC demonstrated the same TGA and DTA curve, thus the corresponding values are discussed in a single diagram as shown in Fig 8.

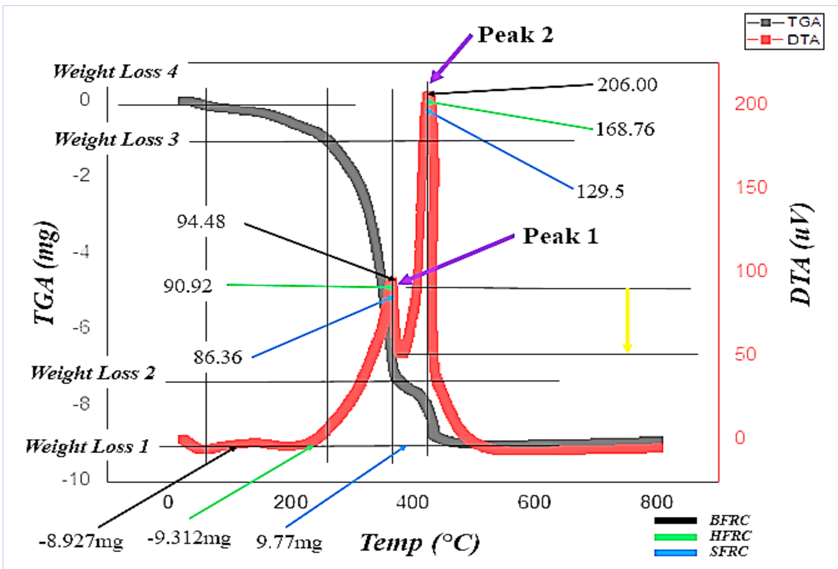

Fig. 8: TGA and DTA curve for SFRC, BFRC, and HFRC

Table 9. TGA and DTA result comparison.

Samples	Weight (mg)	uV		Weight loss			
		Peak 1	Peak 2	Maximum	Loss 3	Loss 2	Minimum
BFRC	10.129	364.54 °C	425.47 °C	8.927 mg	7.290 mg	1.731 mg	0.094 mg
		94.48 uV	206 uV	88.133%	71.972%	17.090%	0.928%
HFRC	10.129	370.18 °C	421.95 °C	9.312 mg	7.752 mg	1.636 mg	0.076 mg
		90.92 uV	168.7 uV	90.329%	75.196%	15.870%	0.737%
SFRC	10.129	376.82 °C	417.5 °C	9.77 mg	8.214 mg	1.541 mg	0.058 mg
		86.36 uV	129.5 uV	96.45%	81.09%	15.21%	0.57%

The TGA curve shows that as the temperature increases, there is a decrease in the weight of all composite samples, which implies there is a mass change continuously due to the thermal effect. As the samples were continually weighed while heating, the BFRC specimens had 4.31% and 9.44% lower mass changes compared to HFRC (9.312 mg weight loss) and SFRC (9.77 mg weight loss) specimens. Table 9 shows that BFRC has superior thermal stability, while SFRC exhibited the highest mass loss, which implies composites with this fiber are less thermally stable. The DTA results further elucidate the thermal behavior of these composites. BFRC absorbed significantly more energy at a temperature of 425.47°C, this indicates a higher thermal energy absorption capacity, potential phase transitions, and substantial thermal degradation at this point. The onset temperature for exothermic reaction for BFRC was 240.33°C which is 4.41% larger compared to SFRC. These temperatures mark the points at which the materials began to release energy typically due to decomposition and chemical reactions. SFRC is the least thermally stable, showing the highest mass loss; in another way, HFRC is not stable as BFRC, but offers a balanced performance with better thermal stability than SFRC and a good onset temperature for exothermic reactions. These findings are crucial for applications requiring materials with robust thermal resistance and stability, highlighting the benefits of using BFRC in thermally demanding environments.

3.6. Main and interaction effect plot

The main effect plot presented in Fig. 9 'a' shows that BFRC had the maximum mean tensile strength, and when the orientation increases from 0 to 90 degree, the mean tensile strength is dramatically increased, which indicates the range of fiber orientation angles which has a potential to significantly influence the corresponding tensile parameters. From the compressive main effect plot diagram it is observed that increasing the fiber orientation angle resulted in decreased mean compressive strength. Figure 9 'b' discloses that all the composites had a significant interaction effect on the mean tensile strength at 0 and 45-degree orientations, and when the orientation angle increases from 45 to 90-degrees, there is no observed interaction effect on the composite tensile strength. Composites with sisal fiber have no significant interaction effect on compressive strength within the range of 0 to 90-degrees fiber orientation. However, bamboo and HFRC exhibited a significant interaction effect on the mean tensile strength at 0 and 90-degree orientations. The main effect plot for BFRC revealed a substantial enhancement in mean tensile strength, indicating a strong positive correlation between fiber alignment and tensile performance. The compressive main effect plot reveals that while tensile strength benefited from increasing fiber alignment angle, the compressive strength was compromised by the same orientation adjustments.

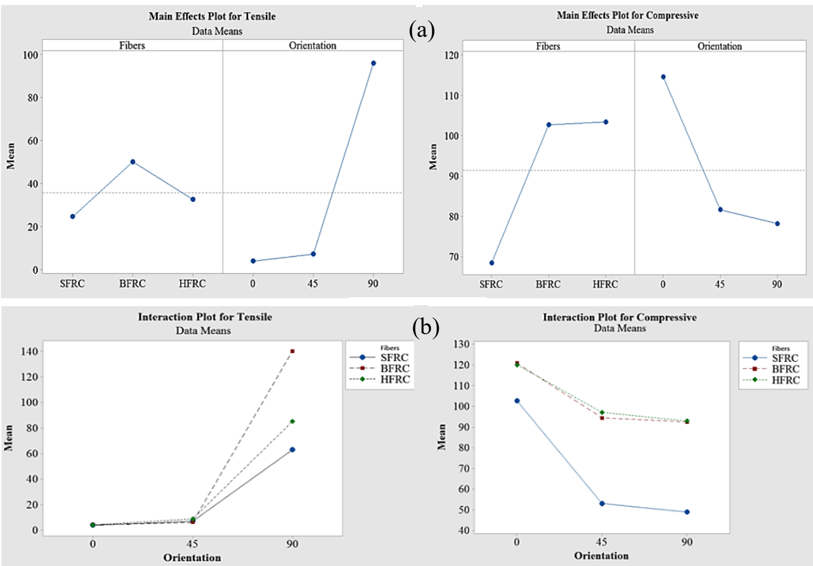

Fig. 9: 'a' Main effect plot 'b' Interaction plot for tensile and compressive strength.

3.7. Macrographic examination

The macrographic examination is a robust and widely accepted method for investigating the fractured surface of a specimen. By employing this method, it became feasible to meticulously observe and analyze the fracture surface of composites. The possible failure modes such as matrix cracks, fiber pull-out, and other failure mechanisms are observed and presented in Fig. 10. The primary objective of the macrographic examination is to discern the underlying causes behind the failure of the sample, thereby contributing to a comprehensive understanding of its behavior and characteristics. Based on the fracture surface analysis of tensile test specimens presented in Fig. 10 (a-c), it is observed that composites with 0-degree orientation demonstrated a delamination fracture mechanism. This group of samples had the perpendicular fiber orientation to the applied load, which enables the matrix material to bear most of the applied load. Consequently, composites in this group exhibited lower tensile strength and brittle failure mode. This is attributed to the fact that the fibers in these composites were easily isolated or segregated. With a 0-degree orientation, the fibers can not contribute significantly to resisting the tensile force applied to the specimen. Composites with a 45-degree orientation demonstrated complex failure modes as shown in Fig. 10 (d-f). Fiber breakage, matrix cracking, fiber pullout, and delamination were the major failure modes observed in this specimen group. The applied tensile load is distributed to the shear and axial components. This resulted in axial stress in fibers and shear stress in the fiber-matrix interface. Composites with 90-degree fiber orientation failed from fiber breakage, which implies that the high strength and stiffness of fibers were fully utilized in this group of samples. As the fibers were aligned in the same direction as the applied load, both fiber and matrix resisted the applied load on the specimen. The fracture surface of HFRC, as depicted in Fig. 10, demonstrated that the SFRC was fractured before the BFRC. This reveals the potential of BFs to withstand more tensile load than SFs.

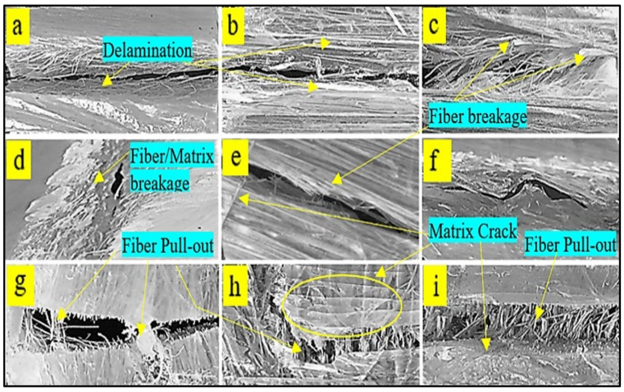

Fig. 10: Fracture surface Macrographic examination of the tensile test specimen 'a' SFRC0, 'b' BFRC0, 'c' HFRC0, 'd' SFRC45, 'e' BFRC45, 'f' HFRC45, 'g' SFRC90, 'h' BFRC90, and 'i' HFRC90

3.8. Multi-response optimization

Grey relational analysis (GRA) in combination with the Taguchi method offers the best optimization approach. This approach is based on the grey theory, which considers the random uncertainty of small samples. Once the experimental results are obtained using the selected suitable OA as shown in Table 10, the steps involved in response optimization include obtaining the normalized values using Eq. 1 and 2, followed by determining the absolute deviation using Eq. 3. Finally, the grey relational coefficient (GRC) and Grey relational grade (GRG) are calculated using Eq. 4 and 5, respectively. The presented results for the flexural and impact strengths are obtained from our previous research work[37].

$$x_{ijk} = \frac{\left((y_{ij}) - \min(y_{ij})\right)}{\max(y_{ij}) - \min(y_{ij})}$$
$$k = 1, 2, 3, \ldots r.\ (\text{Higher is better}) \qquad (1)$$

$$x_{ijk} = \frac{\left(\max(y_{ij}) - (y_{ij})\right)}{\max(y_{ij}) - \min(y_{ij})}$$
$$k = 1, 2, 3, .. r.\ (\text{Lower is better}) \qquad (2)$$

$$\Delta_{ij} = \left|x_{oj} - x_{ijk}\right| \qquad (3)$$

$$\gamma_{(x_{0j}, x_{ij})} = \frac{(\Delta_{min} + \xi\Delta_{max})}{(\Delta_{ij} + \xi\Delta_{max})} \qquad (4)$$

$$\Delta_{min} = \min\{\Delta_{ij}\} \text{ and } \Delta_{max} = \max\{\Delta_{ij}\}$$

The distinguishing coefficient ξ ranges from 0 to 1, with a widely accepted value of 0.5. A smaller ξ indicates higher distinguishability. It serves as a measure of contrast control for the equation. The GRG between the comparability sequence X_i and the reference sequence X_0 is calculated by using Eq. 5.

$$\Gamma_{(X0j, Xij)} = \frac{1}{k \times i}\sum_{i=1}^{n} \gamma_{(x_{0j}, x_{ij})} \quad i = 1, 2, , m \qquad (5)$$

Table 10. Experimental results

Tensile (MPa)	Compressive (MPa)	Impact (kJ/m^2)	Flexural (MPa)	Loss (mg)	Tmax (^oC)
3.83	102.75	23.33	21.88	9.770	417.50
6.92	53.17	30.66	56.25	9.770	417.50
62.92	49.08	43.66	150.0	9.770	417.50
4.08	120.92	22.33	31.25	8.927	425.47
6.00	94.50	28.33	60.00	8.927	425.47
140.17	92.50	41.00	281.25	8.927	425.47
3.99	120.08	23.00	28.125	9.312	421.95
8.75	97.08	33.66	58.125	9.312	421.95
85.08	92.95	46.00	137.50	9.312	421.95

Table 11. Normalization table

Normalized Value						
No	**Tensile**	**Compressive**	**Impact**	**Flexural**	**Weight loss**	**T_{max}**
1	0	0.747077	0.042248	0	0	0
2	0.022664	0.056932	0.351922	0.132513	0	0
3	0.433402	0	0.901141	0.493966	0	0
4	0.001834	1	0	0.036126	1	1
5	0.015916	0.632238	0.253485	0.146972	1	1
6	1	0.604399	0.788762	1	1	1
7	0.001174	0.988307	0.028306	0.024078	0.543298	0.558344
8	0.036086	0.668151	0.478665	0.139742	0.543298	0.558344
9	0.595937	0.610663	1	0.445772	0.543298	0.558344

The normalized value presented in Table 11 is calculated by using Eq. 1 for higher is better and Eq. 2 for lower is better and the corresponding maximum and minimum value is obtained from the normalized responses. Moreover, Table 12 presents the absolute difference between each normalized and the reference value, regardless of the response variable trails, and replications using Eq. 3. Next the grey relational coefficient is obtained using the maximum and minimum of the deviation sequence and by considering the distinguishing coefficient value as 0.5 and employing Eq. 4. Then the average grey relational grade from grey relational coefficient for each level of factors are calculated using Eq. 5. The corresponding values are presented in Table 13.

Table 12. Absolute difference (Deviation Sequence)

No	Tensile	Compressive	Impact	Flexural	Weight loss	T_{max}
1	1	0.252923	0.957752	1	1	1
2	0.977336	0.943068	0.648078	0.867487	1	1
3	0.566598	1	0.098859	0.506034	1	1
4	0.998166	0	1	0.963874	0	0
5	0.984084	0.367762	0.746515	0.853028	0	0
6	0	0.395601	0.211238	0	0	0
7	0.998826	0.011693	0.971694	0.975922	0.456702	0.441656
8	0.963914	0.331849	0.521335	0.860258	0.456702	0.441656
9	0.404063	0.389337	0	0.554228	0.456702	0.441656
Max	**1**	**1**	**1**	**1**	**1**	**1**
Min	**0**	**0**	**0**	**0**	**0**	**0**

Table 13. GRC, GRG, and Rank

No	Grey relational coefficient						GRG	Rank
1	0.333333	0.664078	0.342994	0.333333	0.333333	0.333333	0.39006	8
2	0.338447	0.346484	0.435511	0.365634	0.333333	0.333333	0.35879	9
3	0.46878	0.333333	0.834921	0.497001	0.333333	0.333333	0.46678	7
4	0.333741	1	0.333333	0.341559	1	1	0.66810	2
5	0.336908	0.576195	0.401118	0.369541	1	1	0.61396	3
6	1	0.558284	0.703	1	1	1	**0.87688**	**1**
7	0.333594	0.977149	0.339745	0.338771	0.522629	0.530979	0.50714	5
8	0.34155	0.601071	0.489555	0.367577	0.522629	0.530979	0.47556	6
9	0.553059	0.562216	1	0.474281	0.522629	0.530979	0.60719	4

From Table 13, it has been identified that BFRC90 has optimized as rank one with 0.87688 GRG considering the tensile, compressive, flexural, and impact strength as a larger is better and from thermal analysis lower is better for weight loss and higher is better for temperature peak. The first-ranked composite proved to be an ideal choice for the application requiring higher mechanical properties and good thermal stability. The composites produced by the same bamboo fiber but with a 0-degree orientation

Table 14. Response Table

Response Table		
	Factors	
Level	1	2
1	0.405214	0.52177
2	**0.719649**	0.48277
3	0.529966	**0.65028**

ranked as the second option for the same application. Sisal fiber reinforced composite with 0-degree orientation exhibited the lowest rank with 0.39006 GRG, which is less thermally stable and has a lower mechanical property. From the response Table 14, factor 1 level 2 and factor 2 level 3 have a significant effect on the responses, and factor 1 level 1 has an underrated effect; which indicates that within factor 1, bamboo fiber had a significant effect on the response, while within factor 2, 90-degree orientation had a substantial effect on the response.

3.9. Research's relevance to practical applications

The research explores the mechanical properties of NFRCs, the potential of energy absorption, and mass loss due to the temperature in the composites. This aspect is of great importance in industries where structural integrity and energy dissipation are critical. Understanding the weight loss patterns and thermal degradation characteristics of natural fiber composite material is essential for applications where exposure to high temperatures is expected. This knowledge enables engineers and designers to make informed decisions regarding the suitability of the composites in specific environments, ensuring optimal performance and preventing premature failures. The findings of the mechanical and thermal properties provide valuable information for industries involved in the production of fiber-reinforced composites, empowering them to make thoughtful decisions regarding material selection, processing techniques, and the design of products with enhanced mechanical and thermal properties.

4. Conclusion

This study intended to assess the thermal and mechanical properties of NFRCs. Following the extraction, the fibers underwent alkaline treatment. Nine composites following the L9 orthogonal array were produced. The ideal mixing ratio for UPR and MEKP to complete the fabrication of composites before the matrix cures was determined by preliminary experimental research as 20:1. The interfacial adhesion between the fiber and matrix is found to be effectively improved by the alkali treatment. The optimum mechanical properties of the composites were attained through efficient extraction and treatment methods. The mechanical properties of composites with the same fiber but different orientations and those with the same orientation but different fibers were found entirely distinct. The composites reinforced with bamboo fibers had the highest tensile and compressive strengths when considering the type of fiber used. In another way considering the orientation of fibers, it was found that fibers aligned at 90 degrees exhibited the maximum tensile strength, whereas fibers aligned at 0 degree demonstrated the highest compressive strength. According to the experimental results, the highest compressive and tensile strengths were attained with BFRC0 and BFRC90, respectively. The fiber orientation had a significant effect on the variation of tensile strength. While both factors had an impact on the compressive strength, which was also confirmed by the ANOVA analysis. The ANOVA regression results demonstrated a direct correlation between the tensile strength and fiber ply orientation, but a reverse correlation between the compressive strength and orientation. The BFRC demonstrated lower mass change than the HFRC and SFRC, as determined by continuous heating and sample weighing. With an increase in temperature, oxidation induced an exothermic reaction in all three samples. Bamboo fiber outperforms sisal and hybrid fiber-reinforced composites in terms of thermal stability and energy absorption in both phases. Employing Taguchi-based grey relational analysis and considering higher is better for mechanical properties and thermal stability and lower is better for weight loss, composites with bamboo fiber and 90-degree orientation were optimized as rank 1. The findings of this study will contribute to the applications requiring both higher mechanical strengths and thermal stability; as well as open up new avenues for investigations. Further research on composite coating techniques may prove the potential of these composite materials for extreme environments.

Funding

This research was made possible through the financial support provided by Wolaita Sodo University.

Data availability

The authors confirm that the data supporting the study findings are included in the publication. The corresponding author may provide raw data upon request that back up the study's conclusions.

Conflict of interest

The authors declare that they have no known competing financial interests or personal relationships that could have appeared to influence the work reported in this paper.

Acknowledgments

The authors express their sincere gratitude to Ethiopian Defence University, Addis Ababa University, Adama Science and Technology University, and Wolaita Sodo University for providing the necessary testing equipment and tools.

Ethical approval

Not Applicable

References

1) R. Caliman, "Experimental researches on the tribological analysis of composite materials sintered with iron matrix," *IOP Conference Series: Materials*

Science and Engineering., **591** 012036 (2019). doi:10.1088/1757-899X/591/1/012036.

2) Z. Sun, Y. Duan, H. An, X. Wang, S. Liang, and N. Li, "Research Progress and Application of Natural Fiber Composites," *Journal of Natural Fibers.*, **20** *(2)* (2023). doi:10.1080/15440478.2023.2206591.
3) A. Lotfi, H. Li, D. V. Dao, and G. Prusty, "Natural fiber–reinforced composites: A review on material, manufacturing, and machinability," *Journal of Thermoplastic Composite Materials.,* **34** *(2)* 238–284 (2021). doi:10.1177/0892705719844546.
4) K. Gupta, V. Singhal, and N. Rajput, "Applications and Challenges of Carbon-fibres reinforced Composites: A Review," *Evergreen Joint Journal of Novel Carbon Resource Sciences & Green Asia Strategy.,* **9** (3) 682-693 (2022). doi:10.5109/4843099.
5) M. K. A and R. S, "A Review on natural fiber and its characteristics," *Industrial Engineering Journal.*, **13** *(3)* (2020). doi:10.26488/iej.13.3.1224.
6) S.H. Kamarudin, M.S. Mohd Basri, M. Rayung, F. Abu, S. Ahmad, M.N. Norizan, S. Osman, N. Sarifuddin, et al, "A Review on Natural Fiber Reinforced Polymer Composites (NFRPC) for Sustainable Industrial Applications," *Polymers.,* **14** *(17)* (2022). doi:10.3390/polym14173698.
7) A. Girge, V. Goel, G. Gupta, D. Fuloria, P. R. Pati, A. Sharma, V.K. Mishra, "Industrial waste filled polymer composites – A review," *Mater. Today Proc.,* **47** (2021) doi:10.1016/J.MATPR.2021.03.617.
8) J. Zhang, Z. Yao, K. Wang, F. Wang, H. Jiang, M. Liang, J. Wei, and G. Airey, "Sustainable utilization of bauxite residue (Red Mud) as a road material in pavements, " *Constr. Build. Mater*., **270** 121419 (2021) doi:10.1016/J.CONBUILDMAT.2020.121419.
9) W. Rasemann, "Industrial Wastes and Waste Dumps, Sampling and Analysis," *Encyclopedia of Analytical Chemistry John Wiley & Sons.,* **12** (2015). doi:10.1002/9780470027318.a0831.pub2
10) M. Mallik, S. Hembram, D. Swain, and G. Behera, "Potential utilization of LD slag and waste glass in composite production," *Mater. Today Proc.,* **33** 5196–5199 (2020). doi:10.1016/J.MATPR.2020.02.881.
11) D. Ariawan, W. Raharjo, K. Diharjo, W. Raharjo, and B. Kusharjanta, "Influence of Tropical Climate Exposure on the Mechanical Properties of HDPE Composites reinforced by Zalacca Midrib Fibers," *Evergreen Joint Journal of Novel Carbon Resource Sciences & Green Asia Strategy.,* **9** (3) 662-672(2022). doi:10.5109/4842526.
12) A. Kumar, A.K. Chanda, and S. Angra, "Numerical modeling of a composite sandwich structure having nonmetallic honeycomb core," *Evergreen Joint Journal of Novel Carbon Resource Sciences & Green Asia Strategy.,* **8** (4) 759–767 (2021). doi:10.5109/4742119.
13) V. Ordonez, H. Baykara, A. Riofrio, M. Cornejo, and R. Rodríguez,"Preparation and Characterization of Ecuadorian Bamboo Fiber-Low-Density Polyethylene (LDPE) Biocomposites," *Evergreen Joint Journal of Novel Carbon Resource Sciences & Green Asia Strategy,* **10** (1) 43-54 (2023). doi:10.5109/6781037.
14) Y. G. Thyavihalli Girijappa, S. Mavinkere Rangappa, J. Parameswaranpillai, and S. Siengchin, "Natural Fibers as Sustainable and Renewable Resource for Development of Eco-Friendly Composites: A Comprehensive Review," *Front Mater.,* **6** *226* (2019). doi:10.3389/FMATS.2019.00226/BIBTEX.
15) G. Ekundayo, "Reviewing the Development of Natural Fiber Polymer Composite: A Case Study of Sisal and Jute," *American Journal of Mechanical and Materials Engineering.,* **3** *(1)* 1-10 (2019). doi: 10.11648/j.ajmme.20190301.11.
16) G.S. Mann, N. Azum, A. Khan, M.A. Rub, M.I. Hassan, K. Fatima, A.M. Asiri, "Green Composites Based on Animal Fiber and Their Applications for a Sustainable Future," *Polymers.,* **15** *3* 601 (2023). doi: 10.3390/polym15030601.
17) M. Y. Khalid, A. Al Rashid, Z. U. Arif, W. Ahmed, H. Arshad, and A. A. Zaidi, "Natural fiber reinforced composites: Sustainable materials for emerging applications," *Results in Engineering.,* **11** (2021). doi: 10.1016/j.rineng.2021.100263.
18) A. D. Gudayu, L. Steuernagel, D. Meiners, and A. M. Woubou, "Sisal fiber reinforced polyethylene terephthalate composites; Fabrication, characterization, and possible application," *Polymers and Polymer Composites.,* **30** (2022). doi: 10.1177/09673911221103317.
19) K.V. Akash, R. Sreenivasa, N. S. Venkatesha Gupta, and D. S. Arun Kumar, "Mechanical Properties of Sisal/Coir Fiber Reinforced Hybrid Composites Fabricated by Cold Pressing Method," *IOP Conference Series: Materials Science and Engineering.,* **149** 012092 (2016). doi: 10.1088/1757-899X/149/1/012092.
20) V. Ordonez1, H. Baykara, A. Riofrio, M. Cornejo, and R. Rodríguez, "Preparation and Characterization of Ecuadorian Bamboo Fiber-Low-Density Polyethylene (LDPE) Biocomposites," *Evergreen Joint Journal of Novel Carbon Resource Sciences & Green Asia Strategy.,* **10** *(01)* 43-54 (2023). doi: 10.5109/6781037
21) A. Mofidi, J. Abila, and J. T. M. Ng, "Novel advanced composite bamboo structural members with bio-based and synthetic matrices for sustainable construction," *Sustainability.,* **12** (2020). doi:10.3390/su12062485.
22) P. Lokesh, T. S. A. Surya Kumari, R. Gopi, and G. B. Loganathan, "A study on mechanical properties of bamboo fiber reinforced polymer composite," *Materials Today: Proceedings.*, **22** *(3)* 897–903. doi: 10.1016/j.matpr.2019.11.100.
23) A. Betelie, A. Nicholas Sinclair, M. Kortschot, Y. Li, and D. Tilahun Redda, "Mechanical properties of sisal-epoxy composites as functions of fiber-to-epoxy ratio," *AIMS Mater Sci.*, **6** *(6)* (2019). doi:

10.3934/matersci.2019.6.985.

24) S. Ragunath, N. Shankar, K. Meena, B. Guruprasad, S. Madhu, N. Rakesh, M. Hariprabhu, S. Balamuralitharan and N. Daniel, "Multiobjective Optimization of Mechanical Properties on Sisal-Glass Fiber-Reinforced Hybrid Composites Using Response Surface Methodology and LINGO Analysis," *Advances in Materials Science and Engineering.,* (2021). doi: 10.1155/2021/2376148.
25) C. Wang, Q. Zuo, T. Lin, N.I. Saffinaz Anuar, K.M. Salleh, S. Gan, S. H. Siddique Yousfani, H. Zuo, S. Zakaria, "Predicting thermal conductivity and mechanical property of bamboo fibers/polypropylene nonwovens reinforced composites based on regression analysis," *International Communications in Heat and Mass Transfer.,* **118** 104895 (2020). doi: 10.1016/j.icheatmasstransfer.2020.104895.
26) H.S.A. Embirsh, I. Stajčić, J. Gržetić, I.O. Mladenović, B. Anđelković, A. Marinković, M.M. Vuksanović, "Synthesis, Characterization and Application of Biobased Unsaturated Polyester Resin Reinforced with Unmodified/Modified Biosilica Nanoparticles," *Polymers (Basel).,* **15** *(18)* 3756 (2023). doi: 10.3390/polym15183756.
27) A. M. Sharaf, E. Syala, A. A. Ezzat, S. F. A. Ali, and E. El-Rafey, "Natural Fiber Reinforced Unsaturated Polyester Resin Filled with Bio-based Calcium Carbonate: Preparation and Examination," *Fibers and Polymers.,* **23** *(5)* (2022). doi:10.1007/s12221-022-4460-1.
28) N.I.N. Haris, R.A. Ilyas, M.Z. Hassan, S.M. Sapuan, A. Afdzaluddin, K.R. Jamaludin, S.A. Zaki, "Dynamic mechanical properties and thermal properties of longitudinal basalt/woven glass fiber reinforced unsaturated polyester hybrid composites," *Polymers (Basel).,* **13** (2021). doi:10.3390/polym13193343.
29) W. N. Nkeuwa, J. Zhang, K. E. Semple, M. Chen, Y. Xia, and C. Dai, "Bamboo-based composites: A review on fundamentals and processes of bamboo bonding," *Composites Part B: Engineering.,* **235** (2022). doi:10.1016/j.compositesb.2022.109776.
30) L. Bazli, and M. Bazli, (2021). A review on the mechanical properties of synthetic and natural fiber-reinforced polymer composites and their application in the transportation industry. *Journal of Composites and Compounds.,* **3** *(9)* 262–274 (2021). doi:10.52547/jcc.3.4.6
31) F.I. Mahir, N. K. Keya1, B. Sarker, K. M. Nahiun, A.K. Ruhul, A brief review on natural fiber used as a replacement of synthetic fiber in polymer composites. *Mater Eng Res.*, **1** *(2)* 88-99 (2019).
32) M. Martijanti, A. L. Juwono, and S. Sutarno, "Investigation of characteristics of bamboo fiber for composite structures," *IOP Conf. Ser.: Mater. Sci. Eng.,* **850** 012028 (2020). doi:10.1088/1757-899X/850/1/012028.
33) Y. Dessalegn, B. Singh, A.W.V. Vuure, L.A. Badruddin, H. Beri, M. Hussien, M. Ahmed, G.M.S. Hossain, "Investigation of Bamboo Fibrous Tensile Strength Using Modified Weibull Distribution," *Materials.,* **15** *(14)* 2022. doi: 10.3390/ma15145016.
34) N.G.S. Silva, L.I.C.O. Cortat, and D.R. Mulinari, "Effect of Alkaline Treatment and Coupling Agent on Thermal and Mechanical Properties of Macadamia Nutshell Residues Based PP Composites," *J Polym Environ*., **29** *(10)* 3271–3287 (2021). doi: 10.1007/s10924-021-02112-7.
35) N.M. Nurazzi, M.R.M. Asyraf, M. Rayung, M.N.F. Norrrahim, S.S. Shazleen, M.S.A. Rani, A.R. Shafi, H.A. Aisyah, et al., "Thermogravimetric analysis properties of cellulosic natural fiber polymer composites: A review on influence of chemical treatments," *Polymers.,* **13** *(16)* 2710 (2021). doi: 10.3390/polym13162710.
36) N.M. Nurazzi, N. Abdullah, M.N.F. Norrrahim, S.H. Kamarudin, S. Ahmad, S.S. Shazleen, M. Rayung, R.A. Ilyas, and M. Kuzmin, "Thermogravimetric Analysis (TGA) and Differential Scanning Calorimetry (DSC) of PLA/Cellulose Composites," *Polylactic Acid-Based Nanocellulose and Cellulose Composites, CRC Press.,* (2022). doi: 10.1201/9781003160458-7.
37) M. G. Ganta and M. Patel, "Experimental Comparison of the Effect of Fiber Orientation on Mechanical Properties of Natural Fiber Reinforced Composites (NFRCs)," *Journal of The Institution of Engineers (India): Series D.,* (2023). doi: 10.1007/s40033-023-00520-8.